

# Bortezomib antagonizes microtubule-interfering drug-induced apoptosis by inhibiting G2/M transition and MCL-1 degradation

F Rapino<sup>1</sup>, I Naumann<sup>1</sup> and S Fulda<sup>\*,1</sup>

Inhibition of the proteasome is considered as a promising strategy to sensitize cancer cells to apoptosis. Recently, we demonstrated that the proteasome inhibitor Bortezomib primes neuroblastoma cells to TRAIL-induced apoptosis. In the present study, we investigated whether Bortezomib increases chemosensitivity of neuroblastoma cells. Unexpectedly, we discover an antagonistic interaction of Bortezomib and microtubule-interfering drugs. Bortezomib significantly attenuates the loss of cell viability and induction of apoptosis on treatment with Taxol and different vinca alkaloids but not with other chemotherapeutics, that is, Doxorubicin and Cisplatin. Importantly, Bortezomib inhibits G2/M transition by inhibiting proteasomal degradation of cell cycle regulatory proteins such as p21, thereby preventing cells to enter mitosis, the cell cycle phase in which they are most vulnerable to antitubulin chemotherapeutics. Consequently, Bortezomib counteracts Taxol-induced mitotic arrest and polyploidy, as shown by reduced expression of PLK1 and phosphorylated histone H3. In addition, Bortezomib antagonizes Taxol-mediated degradation of MCL-1 during mitotic arrest by preventing cells to enter mitosis and by inhibiting the proteasome. Downregulation of MCL-1 is critically required for Taxol-induced apoptosis, as overexpression of a phosphomutant MCL-1 variant, which is resistant to degradation, significantly diminishes Taxol-triggered apoptosis. Vice versa, attenuation of Bortezomib-mediated accumulation of MCL-1 by knockdown of MCL-1 significantly enhances Taxol/Bortezomib-induced apoptosis. Thus, Bortezomib rescues Taxol-induced apoptosis by inhibiting G2/M transition and mitigating MCL-1 degradation. The identification of this antagonistic interaction of Bortezomib and microtubule-targeted drugs has important implications for the design of Bortezomib-based combination therapies.

*Cell Death and Disease* (2013) 4, e925; doi:10.1038/cddis.2013.440; published online 21 November 2013

**Subject Category:** Cancer

As the prognosis of neuroblastoma, a common pediatric cancer, remains poor especially for advanced and relapsed disease,<sup>1</sup> new therapeutic approaches are urgently required. Microtubule-interfering drugs are widely used for the treatment of cancer and comprise both vinca alkaloids such as Vincristine, Vinorelbine and Vinblastine that destabilize microtubule formation as well as taxanes such as Taxol that stabilize microtubule formation.<sup>2</sup> The cytotoxic activity of antitubulin chemotherapeutics depends on actively proliferating cells, as they primarily trigger cell death by imposing a mitotic block.<sup>2</sup> Cell cycle progression is precisely regulated in eukaryotic cells and the transition between the different phases of the cell cycle is controlled by transcriptional induction, post translational modifications and proteasomal degradation of various cell cycle-regulatory proteins.<sup>3</sup> Progression through mitosis is intrinsically connected to apoptosis to ensure that cells that exhibit abnormalities during mitosis, for example, prolonged mitotic arrest, are eliminated by programmed cell death. Recently, phosphorylation of the antiapoptotic protein MCL-1 by mitotic kinases and its subsequent proteasomal degradation during prolonged

mitotic arrest, for example, on treatment with antitubulin chemotherapeutics, has been identified as a molecular event that links the failure to resolve mitosis to the initiation of apoptosis.<sup>4,5</sup>

The proteasome is considered as a promising target for anticancer therapy.<sup>6</sup> Bortezomib represents the first proteasome inhibitor approved by the Food and Drug Administration (FDA) for the treatment of human cancers, for example, multiple myeloma and mantle cell lymphoma.<sup>6</sup> Bortezomib is a water-soluble dipeptide boronic acid that reversibly binds to the 26S subunit of the proteasome.<sup>6</sup> Besides its use as monotherapy, Bortezomib has been evaluated as a mean to increase the sensitivity of cancers towards cytotoxic therapies, for example, chemotherapeutic drugs or experimental therapeutics such as the death receptor ligand tumor-necrosis-factor-related apoptosis-inducing ligand (TRAIL).<sup>7,8</sup> Bortezomib has been suggested as a promising investigational drug for neuroblastoma based on its antitumor activity in preclinical studies.<sup>9–15</sup> We recently demonstrated that Bortezomib synergizes with the death receptor ligand TRAIL to trigger apoptosis in preclinical models of neuroblastoma

<sup>1</sup>Institute for Experimental Cancer Research in Pediatrics, Goethe-University Frankfurt, Komturstr. 3a, Frankfurt, Germany

\*Corresponding author: Professor S Fulda, Institute for Experimental Cancer Research in Pediatrics, Goethe-University Frankfurt, Komturstr. 3a, Frankfurt 60528, Germany. Tel: +49 69 67866557; Fax: +49 69 6786659157; E-mail: simone.fulda@kgu.de

**Keywords:** Apoptosis; cell death; Bortezomib; proteasome inhibitor; neuroblastoma

**Abbreviations:** CDK, cyclin-dependent kinase; CI, combination index; FDA, Food and Drug Administration; MTT, 3-(4,5-dimethylthiazol-2-yl)-2,5-diphenyltetrazolium bromide; pH3, phosphorylated histone H3; PI, propidium iodide; PLK1, Polo-like kinase 1; sh, short-hairpin; TRAIL, tumor-necrosis-factor-related apoptosis-inducing ligand; zVAD.fmk, N-benzyloxycarbonyl-Val-Ala-Asp-fluoromethylketone

Received 10.7.13; revised 17.9.13; accepted 01.10.13; Edited by C Munoz-Pinedo

and glioblastoma.<sup>16,17</sup> In the present study, we therefore investigate whether Bortezomib can be used to enhance chemosensitivity of neuroblastoma cells.

## Results

### **Bortezomib rescues neuroblastoma cells from microtubule-targeted drug-induced loss of viability.**

To investigate whether Bortezomib sensitizes neuroblastoma cells to chemotherapy-induced apoptosis, we used SH-EP and LAN5 as cellular models of neuroblastoma that harbor some characteristic genetic alterations of neuroblastoma (Supplementary Table S1). Unexpectedly, we found that Bortezomib significantly attenuated rather than increased Taxol-induced loss of viability over a wide concentration range in both cell lines (Figure 1a). Calculation of combination index (CI) confirmed that the cotreatment of Bortezomib and Taxol is highly antagonistic (Figure 1b). To investigate the effect of Bortezomib on long-term clonogenic survival after treatment with Taxol, we performed colony assays. Importantly, addition of Bortezomib significantly diminished Taxol-mediated reduction of colony formation compared with cells treated with Taxol alone (Figure 1c).

To explore whether the Bortezomib-provided protection against Taxol is a general feature of microtubule-interfering drugs, we extended the experiments to additional drugs that target microtubules, that is, vinca alkaloids. Interestingly, Bortezomib also significantly rescued cell viability upon cotreatment with Vinblastine, Vincristine or Vinorelbine (Figure 1d). In contrast, Bortezomib did not diminish loss of viability on treatment with the topoisomerase II inhibitor Doxorubicin or the DNA-crosslinking agent Cisplatinum (Figure 1e), indicating that Bortezomib-conferred protection against chemotherapy-induced cytotoxicity is stimulus-dependent. Taken together, these results demonstrate that Bortezomib protects neuroblastoma cells against microtubule-interfering drugs.

### **Bortezomib protects against Taxol-induced apoptosis.**

To examine whether Bortezomib-mediated protection is due to inhibition of apoptotic cell death, we measured DNA fragmentation as a characteristic parameter of apoptosis. Importantly, kinetic analysis showed that Bortezomib significantly reduced Taxol-induced DNA fragmentation over an extended time period (Figure 2a). In addition, Bortezomib attenuated Taxol-triggered cleavage of caspase-9 and -3 into active cleavage products compared with treatment with Taxol alone (Figure 2b). Caspase-dependent apoptosis was confirmed by using the pan-caspase inhibitor *N*-benzyloxycarbonyl-Val-Ala-Asp-fluoromethylketone (zVAD.fmk), which significantly reduced DNA fragmentation on treatment with Taxol and/or Bortezomib (Figure 2c). Moreover, we assessed activation of BAX as a marker of mitochondrial apoptosis. Immunoprecipitation followed by western blotting analysis of the active form of BAX revealed that Bortezomib decreased BAX activation in response to Taxol treatment compared with treatment with Taxol alone (Figure 2d). Addition of zVAD.fmk had little effect on BAX activation (Supplementary Figure S1), indicating that BAX activation does not primarily depend on caspase

activity. This set of experiments indicates that Bortezomib rescues cells from Taxol-induced apoptosis.

### **Bortezomib reduces Taxol-induced mitotic arrest.**

Induction of apoptosis by microtubule-targeted drugs has been linked to suppression of microtubule dynamics and prolonged mitotic arrest.<sup>2</sup> As proteasome inhibitors have been described to impair cell cycle progression by disturbing the coordinated degradation of cell cycle regulatory proteins,<sup>6</sup> we asked whether Bortezomib prevents cells from entering mitosis, the phase of the cell cycle in which they are most vulnerable to antitubulin chemotherapeutics. To address this question, we performed cell cycle analysis using flow cytometry. Although treatment with Taxol caused a profound arrest of cells in G2/M phase, the addition of Bortezomib significantly reduced this Taxol-mediated G2/M arrest (Figure 3a). In line with a previous report,<sup>18</sup> treatment with Bortezomib alone increased the amount of cells in G2/M phase (Figure 3a). As flow cytometric analysis of cell cycle distribution does not distinguish between G2 or M phase arrest, we additionally analyzed two M-phase specific markers, that is, Polo-like kinase 1 (PLK1) and phosphorylated histone H3 (pH3).<sup>19,20</sup> Although Taxol markedly enhanced PLK1 and pH3 levels, the addition of Bortezomib substantially reduced this Taxol-stimulated increase of PLK1 and pH3 expression (Figure 3b). As an additional marker of prolonged mitotic arrest and impaired cell division, we quantified the amount of polyploid cells.<sup>21</sup> Notably, the addition of Bortezomib significantly decreased Taxol-stimulated increase in polyploidy (Figure 3c). Consistent with the notion that Bortezomib suppresses cell cycle progression, Bortezomib significantly decreased cell density with little DNA fragmentation compared with untreated cells (Supplementary Figure S2a, Figure 2a).

As cell cycle progression is tightly regulated by the coordinated expression and activity of cyclins, cyclin-dependent kinases (CDKs) and their inhibitors,<sup>3</sup> we hypothesized that Bortezomib-mediated impairment of cell cycle progression is due to stabilization of CDK inhibitor(s). To address this point, we analyzed expression levels of p21 protein as an example of a CDK inhibitor whose stability is tightly controlled by proteasome-mediated degradation.<sup>22</sup> As shown in Figure 3b, Bortezomib caused accumulation of p21 protein with some differences in the kinetics of p21 accumulation in the two cell lines, confirming that Bortezomib alters expression levels of cell cycle regulators in our system. To exclude that Bortezomib interferes with the action of Taxol on its molecular target, we analyzed the acetylation status of tubulin, a marker of microtubule stabilization.<sup>2</sup> Bortezomib did not alter Taxol-stimulated increase in acetylated tubulin (Supplementary Figure S2b), indicating that Bortezomib does not interfere with Taxol's effect on microtubule dynamics. Together, this set of experiments shows that Bortezomib impairs Taxol-induced G2/M transition, mitotic arrest and induction of polyploidy.

### **Schedule-dependent protection against Taxol-induced apoptosis by Bortezomib.**

To further test the hypothesis that Bortezomib rescues Taxol-induced apoptosis by interfering with Taxol-induced mitotic arrest, we added

Bortezomib simultaneously or, alternatively, at 2, 6 or 12 h after administration of Taxol. Interestingly, increasing the time gap between the addition of Bortezomib and the administration of Taxol resulted in a progressive loss of Bortezomib's ability to protect against Taxol-induced apoptosis (Figure 4a). In parallel, the ability of Bortezomib to inhibit Taxol-induced

mitotic arrest and induction of polyploidy was lost or substantially impaired, when it was added 12h after Taxol (Figures 4b–d). These results reveal that the Bortezomib-conferred protection against Taxol-induced apoptosis is schedule-dependent and confirm that Bortezomib rescues Taxol-induced apoptosis by impairing cell cycle progression.

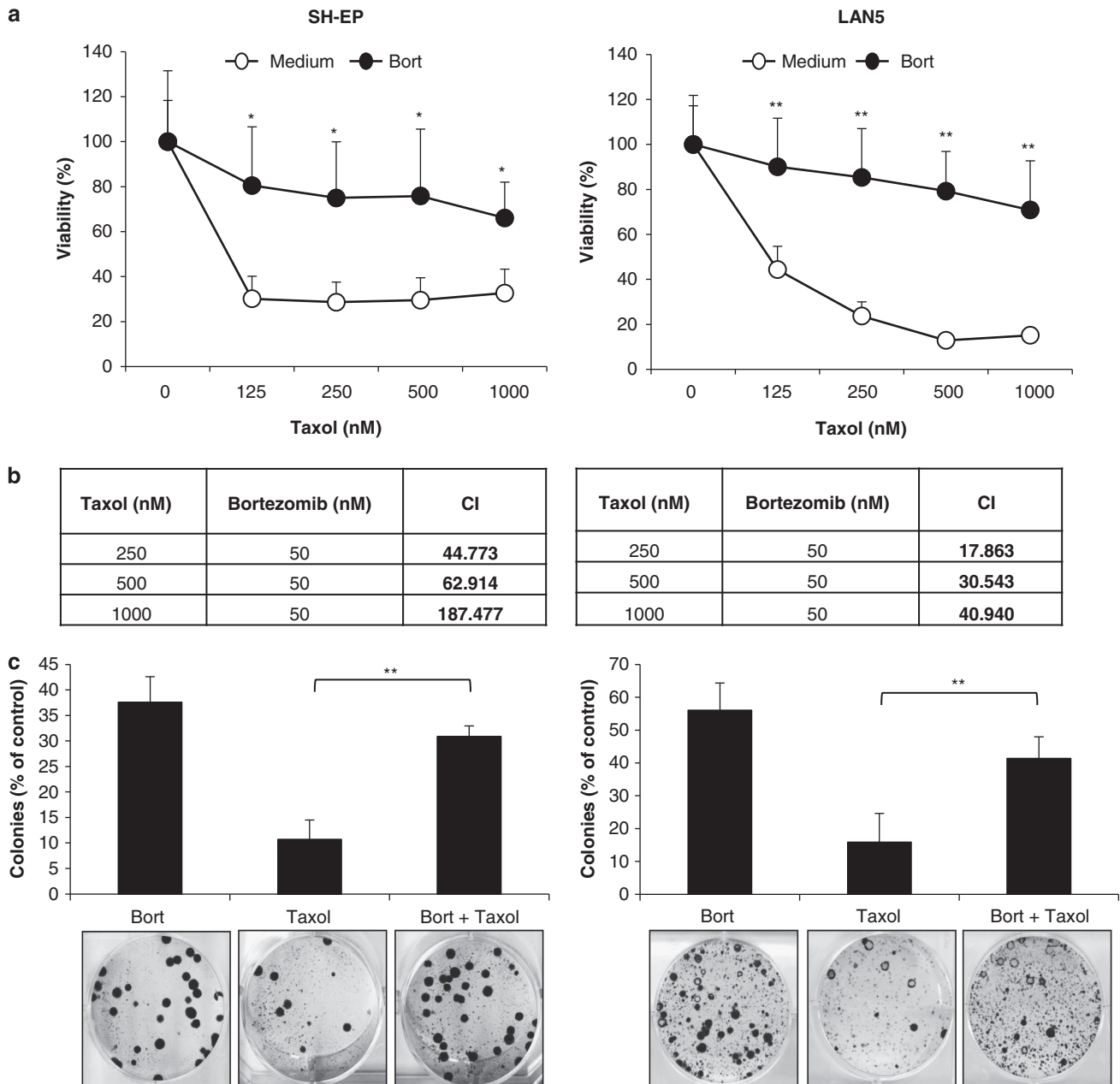


**Figure 1** Bortezomib rescues neuroblastoma cells from Taxol-induced loss of viability. (a and b) SH-EP and LAN5 cells were treated with indicated concentrations of Taxol and/or 50 nM Bortezomib for 24 and 36 h, respectively. Cell viability was assessed by MTT assay and is expressed as the percentage of controls (a). CI was determined by the CalcuSyn software (b). CI < 0.9 indicates synergism, 0.9–1.1 additivity and > 1.1 antagonism. (c) SH-EP and LAN5 cells were treated with 1  $\mu$ M Taxol and/or 50 nM Bortezomib for 24 and 36 h, respectively; then cells were seeded as single cells and grown in drug-free medium for 14 days before colony formation was assessed by crystal violet staining and colonies were counted under the microscope. The number of colonies is expressed as the percentage of untreated controls (upper panels) and representative images are shown (lower panels). (d) SH-EP and LAN5 cells were treated with indicated concentrations of Vinblastine, Vincristine and Vinorelbine and/or 50 nM Bortezomib for 24 and 36 h, respectively. Cell viability was assessed by MTT assay and is expressed as the percentage of untreated controls. (e) SH-EP cells were treated with indicated concentrations of Doxorubicin or Cisplatin and/or 50 nM Bortezomib for 24 h. Cell viability was assessed by MTT assay and is expressed as the percentage of untreated controls. Mean + S.D. of three independent experiments performed in triplicate are shown; \* $P$  < 0.05; \*\* $P$  < 0.01

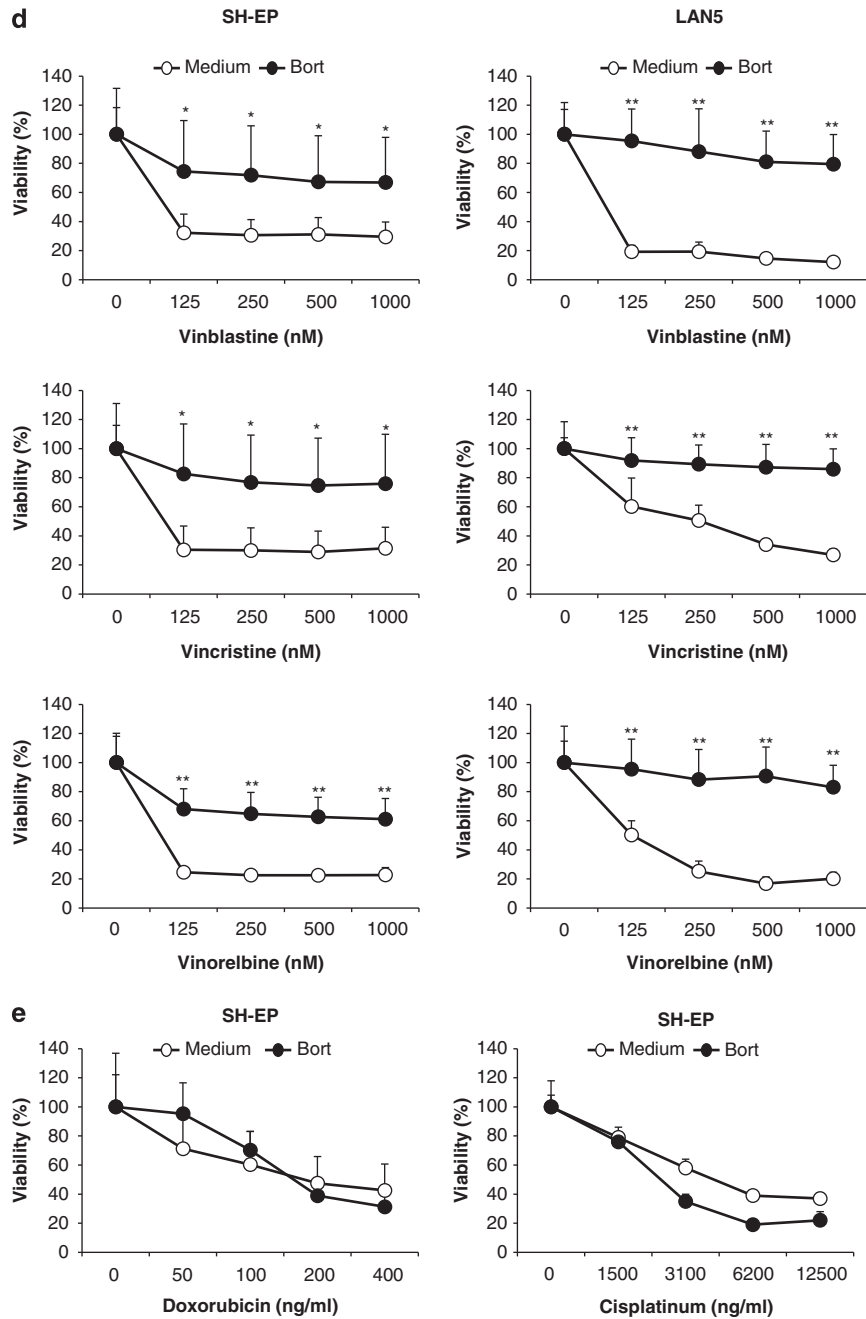
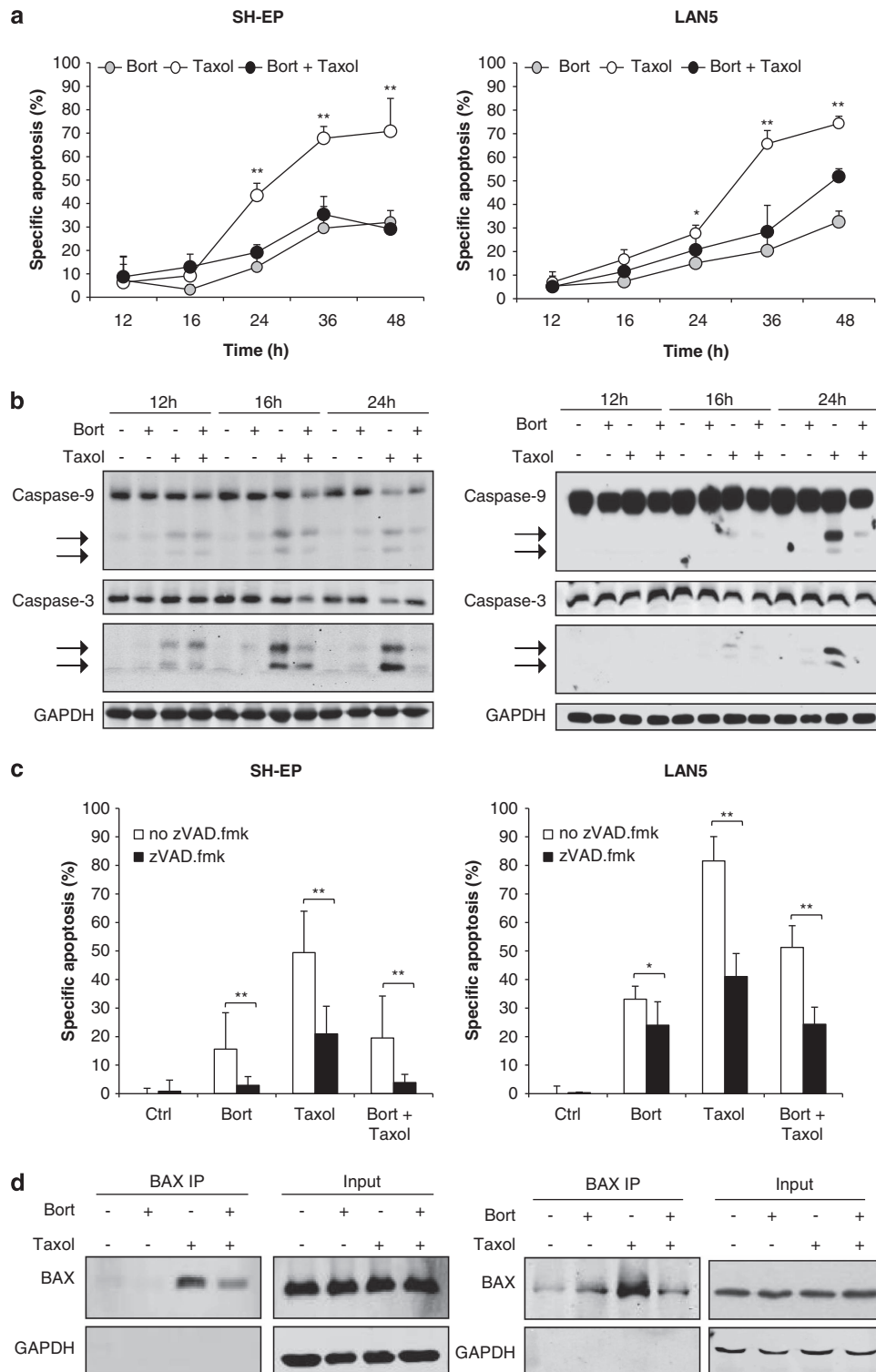


Figure 1 Continued

**Bortezomib counteracts Taxol-stimulated MCL-1 degradation and BCL-2 phosphorylation.** Antitubulin chemotherapeutics have been reported to modulate expression levels and post translational modifications of two antiapoptotic BCL-2 family proteins, that is, MCL-1 and BCL-2, during mitotic arrest.<sup>4,23</sup> Proteasomal degradation of MCL-1 has been described to be required for microtubule-targeted drug-induced apoptosis,<sup>4</sup> while phosphorylation of BCL-2 during mitotic arrest has been reported as a pro apoptotic or antiapoptotic event depending on the context.<sup>24</sup> In addition, BCL-2 has been implicated in the control of cell cycle progression.<sup>25</sup> Therefore, we monitored

expression and phosphorylation of MCL-1 and BCL-2 on treatment with Taxol and/or Bortezomib. Interestingly, Bortezomib abolished the Taxol-triggered progressive decline of MCL-1 protein levels (Figure 5). Also, treatment with Bortezomib alone caused accumulation of MCL-1 protein compared with untreated cells (Figure 5), which is likely due to its reduced proteasomal degradation upon Bortezomib treatment. Furthermore, Bortezomib profoundly suppressed Taxol-stimulated phosphorylation of BCL-2 (Figure 5). Notably, the ability of Bortezomib to counteract Taxol-mediated MCL-1 degradation or BCL-2 phosphorylation was substantially impaired, when it was added 12 h after



**Figure 2** Bortezomib impairs Taxol-induced apoptosis. SH-EP and LAN5 cells were treated with 1  $\mu$ M Taxol and/or 50 nM Bortezomib for the indicated time points. (a) Apoptosis was determined by analysis of DNA fragmentation of PI-stained nuclei using flow cytometry. Mean + S.D. of three independent experiments performed in triplicate are shown; \* $P < 0.05$ ; \*\* $P < 0.01$ . (b) Activation of caspase-9 and -3 was detected by western blotting analysis, arrowheads indicate cleavage products. GAPDH (glyceraldehyde 3-phosphate dehydrogenase) was used as loading control. (c) SH-EP and LAN5 cells were treated for 24 and 36 h, respectively, with 1  $\mu$ M Taxol and/or 50 nM Bortezomib in the presence or absence of 20  $\mu$ M zVAD.fmk. Apoptosis was determined by DNA fragmentation of PI-stained nuclei and flow cytometry. Mean + S.D. of three independent experiments performed in triplicate are shown; \* $P < 0.05$ ; \*\* $P < 0.01$ . (d) SH-EP and LAN5 cells were treated with 1  $\mu$ M Taxol and/or 50 nM Bortezomib for 24 h. The active form of BAX was immunoprecipitated from total protein lysates. BAX protein levels were detected by western blotting. GAPDH was used as purity and loading control

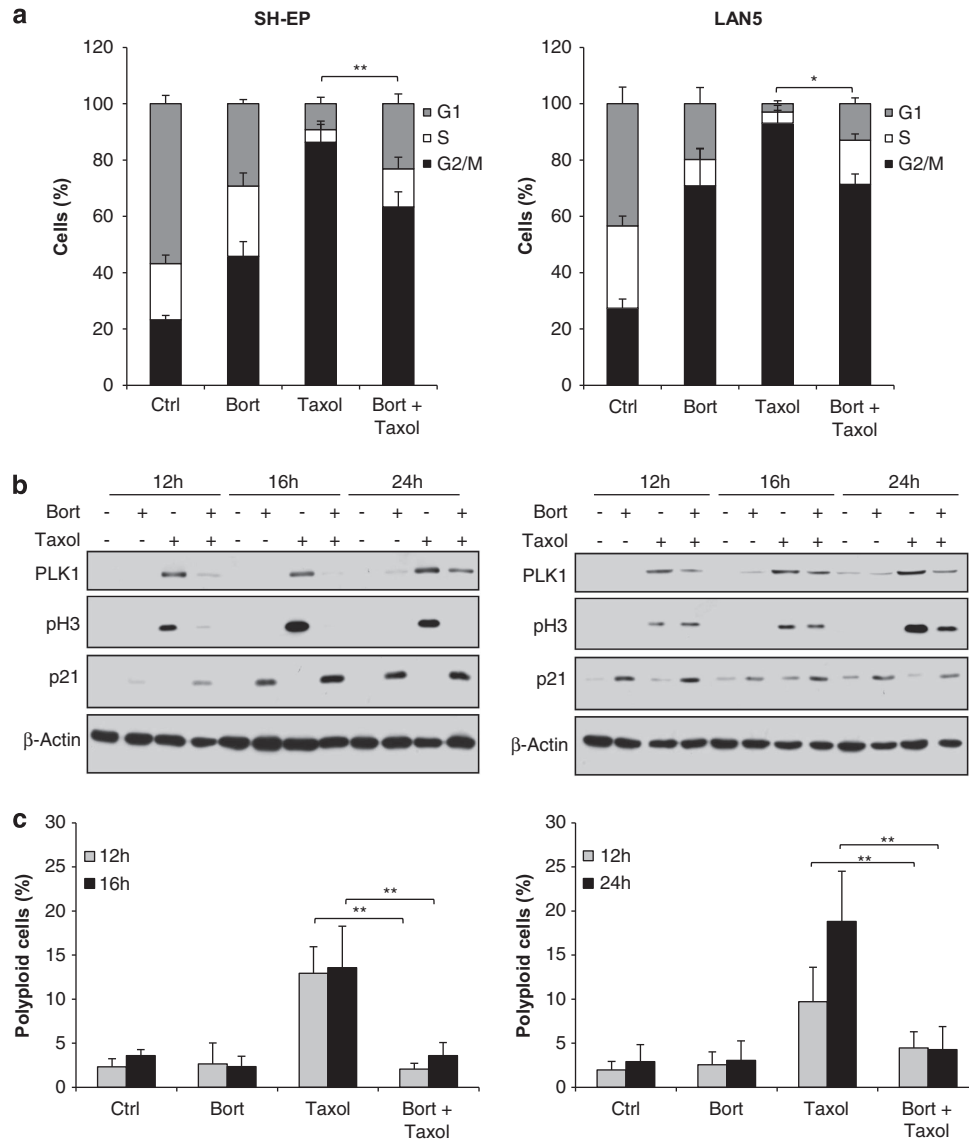


**Figure 3** Bortezomib decreases Taxol-induced G2 arrest. (a) SH-EP and LAN5 cells were treated with 1  $\mu$ M Taxol and/or 50 nM Bortezomib for 16 and 24 h, respectively. DNA was stained by PI, and cell cycle analysis was performed by flow cytometry and FlowJo software. Mean  $\pm$  S.D. of three independent experiments performed in triplicate are shown; \* $P$  < 0.05; \*\* $P$  < 0.01. (b) SH-EP and LAN5 cells were treated with 1  $\mu$ M Taxol and/or 50 nM Bortezomib for the indicated time points. PLK1, pH3 and p21 protein levels were detected by western blotting analysis.  $\beta$ -Actin was used as the loading control. (c) SH-EP and LAN5 cells were treated with 1  $\mu$ M Taxol and/or 50 nM Bortezomib for the indicated time points. DNA was stained by PI, and the percentage of polyloid cells was evaluated by FlowJo software analysis. Mean  $\pm$  S.D. of three independent experiments performed in triplicate are shown; \* $P$  < 0.05; \*\* $P$  < 0.01

Taxol (Supplementary Figure S3), in parallel with its failure to rescue Taxol-induced mitotic arrest and apoptosis under these conditions (Figures 4a–c). This set of data demonstrates that Bortezomib inhibits the Taxol-triggered proteasomal degradation of MCL-1 and phosphorylation of BCL-2.

**BCL-2 phosphorylation rescues Taxol-induced apoptosis by modulating the cell cycle.** To investigate the role of BCL-2 phosphorylation, we generated SH-EP cells overexpressing BCL-2 wild-type (BCL-2 WT), BCL-2 phosphomutant (BCL-2 AAA), which cannot be phosphorylated during mitotic arrest, and BCL-2 phosphomimetic (BCL-2 EEE), which mimics the effect of phosphorylation

(Supplementary Figure S4a).<sup>23</sup> Interestingly, cells expressing BCL-2 phosphomutant (BCL-2 AAA) exhibited increased PLK1 levels and G2/M arrest upon Bortezomib/Taxol cotreatment compared with cells expressing BCL-2 WT (Figure 6a lanes 4 and 8; Figure 6b, right panel). Consistently, Bortezomib/Taxol-induced apoptosis was significantly increased in BCL-2 phosphomutant cells compared with BCL-2 WT (Figure 6c). This demonstrates that impairment of BCL-2 phosphorylation leads to increased mitotic arrest and apoptosis. On the contrary, BCL-2 phosphomimetic cells (BCL-2 EEE) displayed decreased PLK1 levels and G2/M arrest upon Taxol treatment compared with BCL-2 WT cells (Figure 6a lanes 3 and 15; Figure 6b, left panel). In

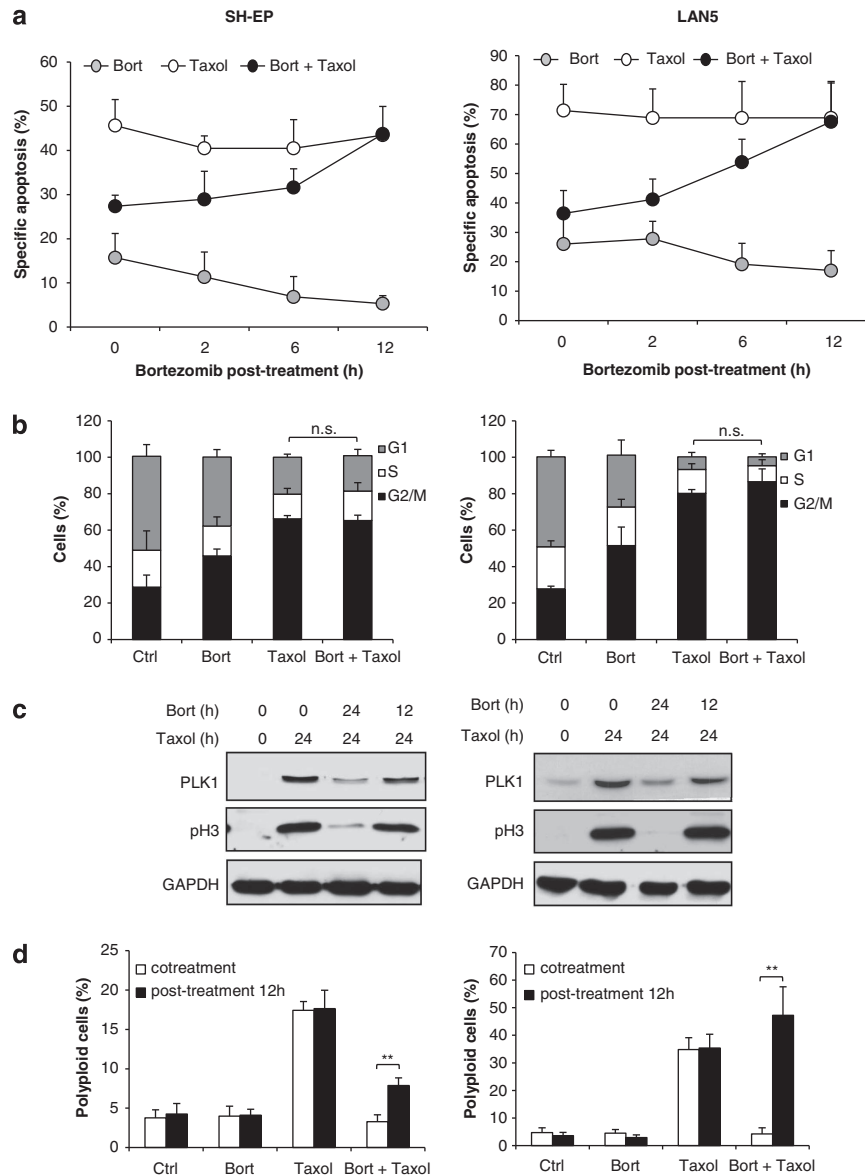


**Figure 4** Schedule-dependent protection against Taxol-induced apoptosis by Bortezomib. (a) SH-EP and LAN5 cells were treated with 1  $\mu$ M Taxol for 24 and 36 h, respectively. A total of 50 nM Bortezomib was added at indicated time points. Apoptosis was determined by the analysis of DNA fragmentation of PI-stained nuclei and flow cytometry. Mean  $\pm$  S.D. of three independent experiments performed in triplicate are shown. (b) SH-EP and LAN5 cells were treated with 1  $\mu$ M Taxol for 24 h, and 50 nM Bortezomib was added after 12 h. DNA was stained by PI, and the cell cycle analysis was performed by flow cytometry and FlowJo software. Mean  $\pm$  S.D. of three independent experiments performed in triplicate are shown; NS, not significant. (c and d) SH-EP and LAN5 cells were treated with 1  $\mu$ M Taxol for 24 h, and 50 nM Bortezomib was added concomitantly or after 12 h. PLK1 and pH3 protein levels were assessed by western blotting analysis; GAPDH (glyceraldehyde 3-phosphate dehydrogenase) was used as the loading control (c). DNA was stained by PI and the percentage of polyloid cells was determined by flow cytometry and FlowJo software analysis (d). Mean  $\pm$  S.D. of three independent experiments performed in triplicate are shown; \*\* $P < 0.01$

line with this attenuation of Taxol-induced mitotic arrest in BCL-2 EEE cells, these cells were significantly protected against Taxol-induced apoptosis (Figure 6c). By comparison, these BCL-2 variants exhibited similar cell cycle profiles under constitutive conditions or upon Bortezomib treatment (Supplementary Figure S4b). This set of experiments indicates that BCL-2 phosphorylation is an antiapoptotic event during Taxol-induced apoptosis by impairing cell cycle progression and mitotic arrest. This implies that Bortezomib-mediated suppression of Taxol-stimulated

BCL-2 phosphorylation is the consequence of reduced mitotic arrest rather than the cause of the Bortezomib-conferred protection against apoptosis.

**Bortezomib rescues Taxol-induced apoptosis by counteracting MCL-1 degradation.** To investigate the role of MCL-1 in Bortezomib-mediated protection against Taxol-induced apoptosis, we used the following genetic approaches. First, we overexpressed a phosphomutant variant of MCL-1 (Myc-MCL-1 4A), which is insensitive to

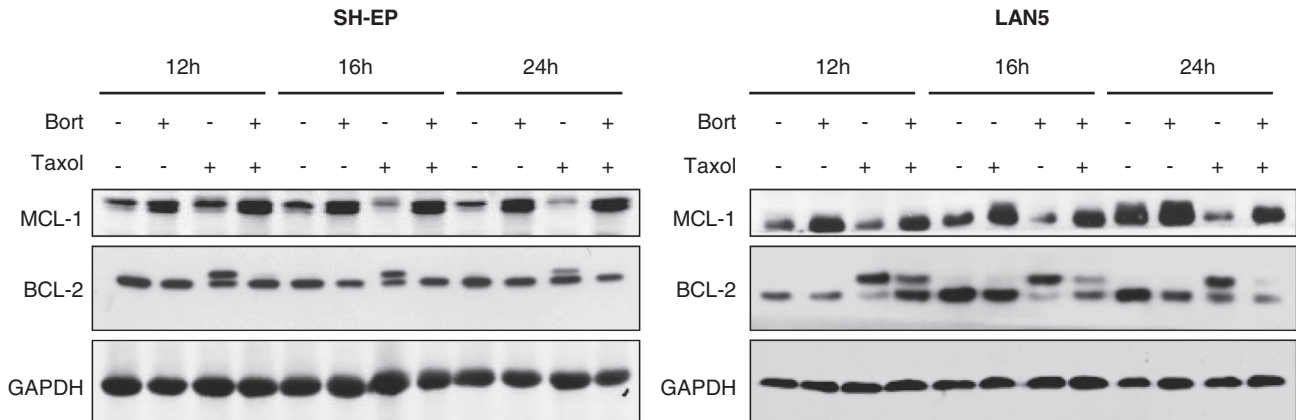


**Figure 5** Bortezomib counteracts Taxol-triggered MCL-1 degradation and BCL-2 phosphorylation. SH-EP and LAN5 cells were treated with 1  $\mu$ M Taxol and/or 50 nM Bortezomib for the indicated time points. MCL-1 and BCL-2 protein levels were assessed by western blotting analysis. GAPDH (glyceraldehyde 3-phosphate dehydrogenase) was used as loading control

Taxol-induced proteasomal degradation<sup>4</sup> (Figure 7a). Second, we stably knocked down MCL-1 by short-hairpin (sh) RNA interference (Figure 7c). Third, we transiently knocked down MCL-1 by short interfering (si) RNA (Figure 7e). Importantly, ectopic expression of MCL-1 phosphomutant (Myc-MCL-1 4A) prevented the Taxol-induced downregulation of MCL-1 protein and significantly decreased Taxol-induced apoptosis compared with cells transfected with MCL-1 wild-type (Myc-MCL-1 WT) (Figure 7b). Vice versa, interference with Bortezomib-triggered accumulation of MCL-1 by shRNA or siRNA resulted in a significant increase in Taxol/Bortezomib- or Bortezomib-induced apoptosis (Figures 7d and f). This set of results indicates that Bortezomib-triggered accumulation of MCL-1 contributes to Bortezomib-conferred protection against Taxol-induced apoptosis.

## Discussion

Concomitant targeting of different cellular pathways is considered as a promising strategy in tumor treatment. For example, the FDA-approved proteasome inhibitor Bortezomib has been used in combination regimens to enhance the antitumor activity of various cytotoxic drugs.<sup>8</sup> We recently showed that Bortezomib synergizes with the death receptor ligand TRAIL in preclinical models of neuroblastoma and glioblastoma.<sup>16,17</sup> In the present study, we therefore asked whether Bortezomib can be used to enhance the chemosensitivity of neuroblastoma cells.

Unexpectedly, we discover an antagonistic drug interaction of Bortezomib and microtubule-interfering drugs, including Taxol and vinca alkaloids. We demonstrate that Bortezomib impairs Taxol-mediated apoptosis, as confirmed by several parameters of apoptotic cell death, that is, reduced DNA fragmentation, BAX activation, caspase cleavage and caspase-dependent cell death. The relevance of our findings is underlined by experiments showing that Bortezomib restores long-term clonogenic survival after Taxol treatment. We propose a model in which the proteasome inhibitor Bortezomib inhibits G2/M transition by disturbing the coordinated degradation of cell cycle regulatory proteins, thereby

preventing cells to enter mitosis, the cell cycle phase in which they are most vulnerable to microtubule-targeted drugs (Figure 8). Several lines of evidence support this conclusion. First, cotreatment with Bortezomib mitigates Taxol-induced mitotic arrest as shown by the lower percentage of cells in M phase, reduced expression of mitotic markers such as PLK1 and pH3 and a decrease in polyploidy upon cotreatment. Modification of the schedule of Bortezomib administration underscores the critical role of cell cycle events for the antagonistic drug interaction, as addition of Bortezomib 12 h after Taxol treatment abrogates its ability both to interfere with Taxol-stimulated mitotic arrest and to rescue cells from Taxol-induced apoptosis. Second, in line with the proposed mechanism of action, Bortezomib selectively protects against microtubule-interfering drugs but not against other classes of chemotherapeutic agents, that is, the topoisomerase II inhibitor Doxorubicin or the DNA-crosslinking agent Cisplatin. Third, Bortezomib antagonizes the Taxol-mediated proteasomal degradation of MCL-1 during mitotic arrest, both by preventing cells to enter mitosis and by inhibiting the proteasome. This Bortezomib-mediated blockage of Taxol-stimulated depletion of MCL-1 contributes to the rescue effect of Bortezomib as shown by the following two sets of experiments: (I) Similar to co-administration of Bortezomib, the genetic inhibition of Taxol-induced downregulation of MCL-1 by ectopic expression of a phosphomutant variant of MCL-1, which cannot be phosphorylated and thus marked for proteasomal degradation, significantly reduces Taxol-induced apoptosis. (II) Abolishing the Bortezomib-mediated accumulation of MCL-1 by genetic silencing significantly increases apoptosis upon Taxol/Bortezomib cotreatment. Thus, proteasomal degradation of MCL-1 represents a critical event that links Taxol-stimulated mitotic arrest to the induction of apoptosis.

Proteasomal degradation of MCL-1 on its phosphorylation during prolonged mitotic arrest was recently identified as a key step during apoptosis on treatment with microtubule-interfering drugs.<sup>4,5</sup> Importantly, we demonstrate in this study that Bortezomib counteracts Taxol-stimulated proteasomal degradation of MCL-1, thereby providing protection against a distinct class of anticancer drugs, that is, antitubulin



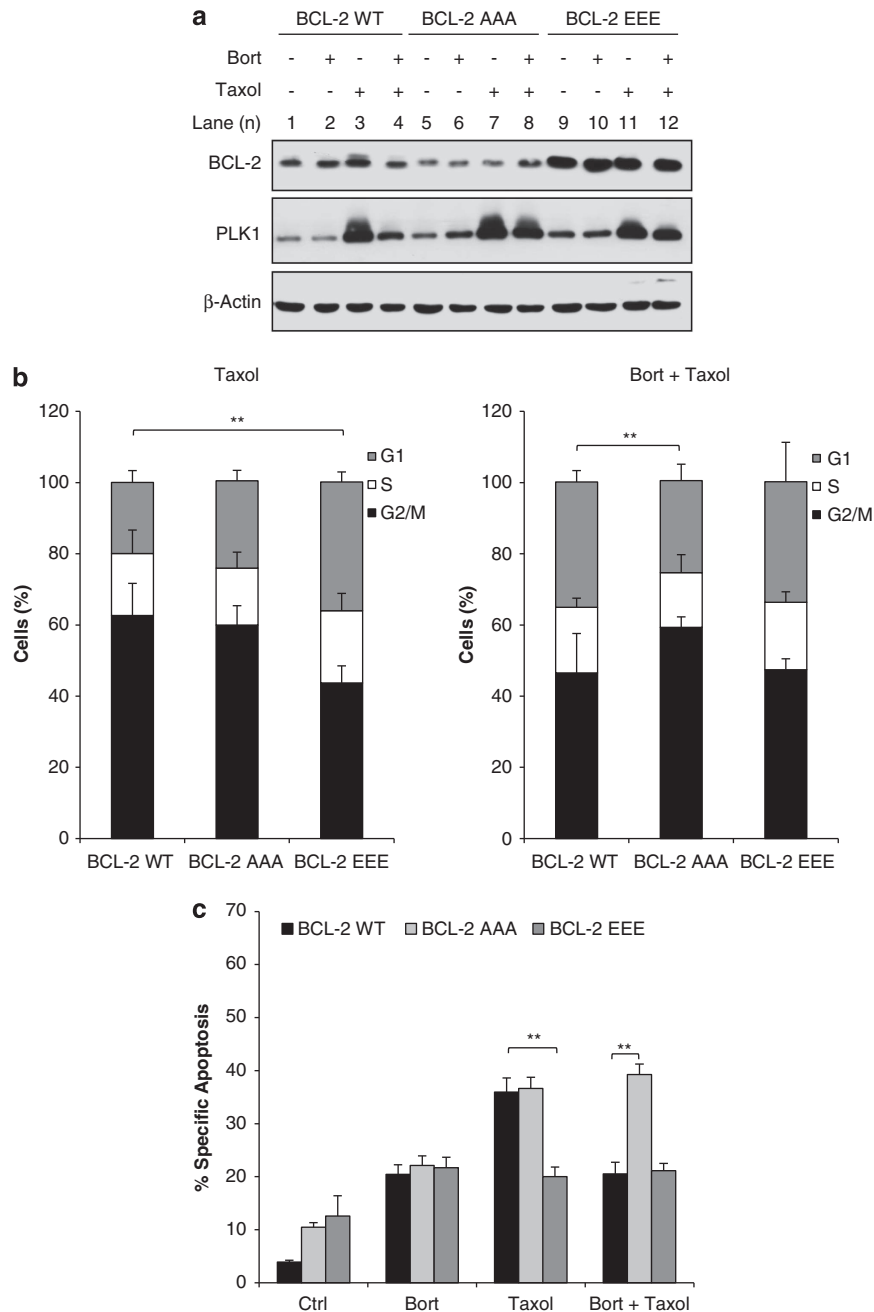


**Figure 6** BCL-2 phosphorylation rescues Taxol-induced apoptosis by modulating the cell cycle. SH-EP cells were transfected with BCL-2 wild-type (BCL-2 WT), BCL-2 phosphomutant (BCL-2 AAA) and BCL-2 phosphomimetic plasmid (BCL-2 EEE) and treated for 24 h with 1  $\mu$ M Taxol and/or 50 nM Bortezomib. Expression of ectopically expressed murine BCL-2 and PLK1 levels was detected by western blotting analysis;  $\beta$ -Actin was used as the loading control (a). Cell cycle analysis was performed by DNA staining with PI, flow cytometry and FlowJo software (b). Apoptosis was determined by the analysis of DNA fragmentation of PI-stained nuclei and flow cytometry (c). Mean  $\pm$  S.D. of three independent experiments performed in triplicate are shown; \*\* $P < 0.01$

chemotherapeutics that exert their cytotoxicity during mitosis. In contrast to MCL-1 phosphorylation, which we demonstrate to be critically required for Taxol-induced apoptosis, the Taxol-stimulated phosphorylation of BCL-2 represents an antiapoptotic event during Taxol-mediated apoptosis. Using both a phosphomutant and a phosphomimetic variant of BCL-2, our data indicate that BCL-2 phosphorylation is a consequence of Taxol-induced mitotic arrest and inhibits

apoptosis by attenuating cell cycle progression to the M phase, in line with previous reports showing that BCL-2 blocks apoptosis by inhibiting cell cycle progression.<sup>25,26</sup>

Proteasome inhibitors have been described to inhibit cell cycle progression by disturbing the coordinated degradation of cell cycle regulatory proteins.<sup>18</sup> However, the impact of Bortezomib on Taxol-induced apoptosis has been controversially discussed. Although Bortezomib was shown to increase

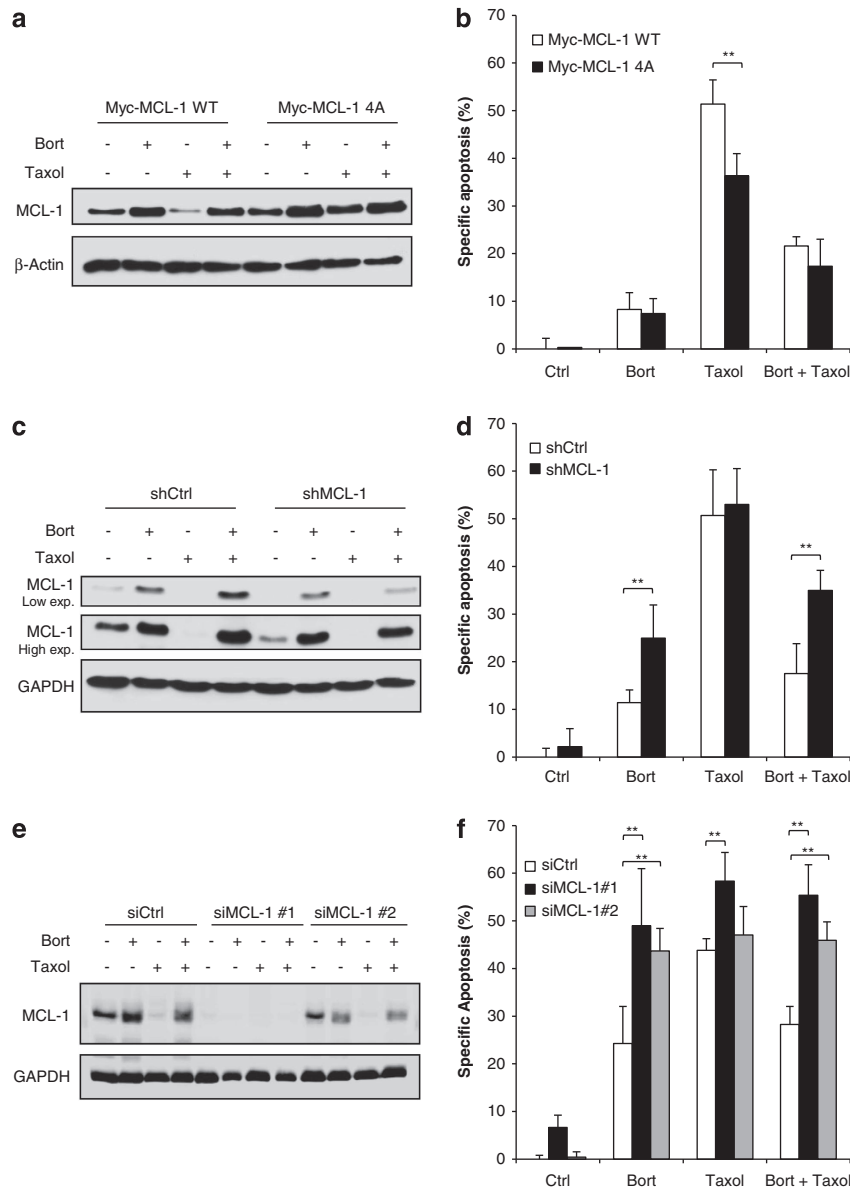


**Figure 7** Bortezomib rescues Taxol-induced apoptosis by counteracting MCL-1 degradation. (a and b) SH-EP cells were transfected with MCL-1 wild-type (Myc-MCL-1 WT) or MCL-1 phosphomutant plasmid (Myc-MCL-1 4A) and treated for 24 h with 1  $\mu$ M Taxol and/or 50 nM Bortezomib. Expression of MCL-1 was detected by western blotting analysis,  $\beta$ -actin was used as loading control (a). Apoptosis was determined by the analysis of DNA fragmentation of PI-stained nuclei and flow cytometry (b). (c and d) SH-EP cells transduced with control vector (shCtrl) or vector containing shRNA sequence against MCL-1 (shMCL-1) were treated for 24 h with 1  $\mu$ M Taxol and/or 50 nM Bortezomib. Expression of MCL-1 was detected by western blotting analysis, GAPDH (glyceraldehyde 3-phosphate dehydrogenase) was used as loading control (c). Apoptosis was determined by the analysis of DNA fragmentation of PI-stained nuclei and flow cytometry (d). (e and f) SH-EP cells transfected with 5 nM siMCL-1 and treated for 24 h with 1  $\mu$ M Taxol and/or 50 nM Bortezomib. Expression of MCL-1 was detected by western blotting analysis, GAPDH was used as loading control (e). Apoptosis was determined by the analysis of DNA fragmentation of PI-stained nuclei and flow cytometry (f). In (b), (d) and (f), mean  $\pm$  S.D. of three independent experiments performed in triplicate are shown; \*\* $P < 0.01$

apoptosis on treatment with Taxol in lymphoma or pancreatic carcinoma cells,<sup>27,28</sup> another study reported that it decreased Taxol-mediated apoptosis of ovarian carcinoma cells.<sup>29</sup> Thus, cell type-dependent factors may contribute to the regulation of Taxol-induced apoptosis by Bortezomib.

Our findings have important implications for the use of Bortezomib in combination therapies for the treatment of cancers such as neuroblastoma, especially as Bortezomib in combination with chemotherapeutics, including taxanes, is being evaluated in clinical trials<sup>30</sup> (<http://www.clinical>

trials.gov). By identifying antagonistic drug interactions under certain conditions, that is, when Bortezomib is combined with microtubule-interfering drugs in neuroblastoma cells, our study challenges the concept that Bortezomib functions as 'universal' sensitizer for apoptosis, as previously shown for certain combinations such as Bortezomib plus TRAIL.<sup>8,16,17</sup> Rather, Bortezomib modulates apoptosis sensitivity of cancer cells in a context-dependent manner, depending on, for example, the cytotoxic stimulus, cell type, administration schedule and so on. Notably, we show that altered

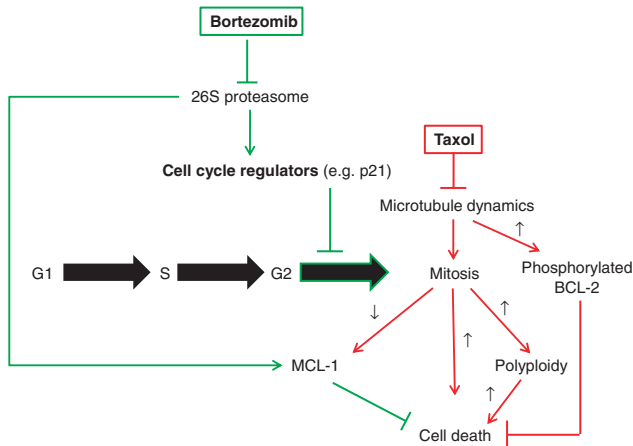


**Figure 8** Scheme of the proposed mechanism. Taxol inhibits microtubule dynamics and induces prolonged mitotic arrest, which leads to proteasomal degradation of MCL-1 and polyploidy and eventually to apoptosis (red lines). Bortezomib inhibits G2/M transition and blocks proteasomal degradation of MCL-1 (green lines), thereby impairing Taxol-induced cell death. See text for details

administration of Bortezomib 12 h after Taxol completely abrogates its ability to rescue Taxol-stimulated mitotic arrest and apoptosis, underscoring the concept of context dependency. Therefore, preclinical evaluation of Bortezomib-based combinations in a given tumor type as well as studies of the underlying mechanisms of drug interaction and of the most suitable administration schedule are critical for the rational design of synergistic combination therapies with Bortezomib for clinical translation.

## Materials and Methods

**Cell culture and chemicals.** Neuroblastoma cell lines were obtained from the American Type Culture Collection (Manassas, VA, USA). Cells were maintained in DMEM medium (Life Technologies, Inc., Eggenstein, Germany), supplemented with 10% fetal calf serum (Biochrom, Berlin, Germany), 1 mM glutamine (Invitrogen, Karlsruhe, Germany), 1% penicillin/streptomycin (Invitrogen) and 25 mM HEPES (Biochrom). Bortezomib was obtained from Jansen-Cilag (Neuss, Germany); Doxorubicin, Taxol, Vinblastine, Vincristine, Vinorelbine and Cisplatin from Sigma (Deisenhofen, Germany). zVAD.fmk was obtained from Bachem (Heidelberg, Germany). BCL-2 plasmids (pCIneo; BCL-2 WT, BCL-2 AAA, BCL-2 EEE) were kindly provided by Professor W.S. May (Gainesville, FL, USA), MCL-1 plasmids (Myc-MCL-1 WT, Myc-MCL-1 4A (S64A/S121A/S159A/T163A)) by Genentech (South San Francisco, CA, USA). Chemicals were purchased from Sigma unless otherwise indicated.

**Cell transduction and transfection.** For stable gene knockdown, shRNA targeting MCL-1 sequence (5'-GGCAGTCGCTGGAGATTAT-3') or a control sequence with no corresponding part in the human genome (5'-GATCATGTAGATACGCTCA-3') were cloned into pGreenPuro, and lentivirus-containing supernatants were generated as previously described.<sup>31</sup> Stable cell lines were produced by selection with 1  $\mu$ g/ml puromycin. Cells were transfected with 4  $\mu$ g of plasmid supplied with Lipofectamine 2000 (Invitrogen); BCL-2 EEE (T69E/S70E/S87E); BCL-2 AAA (T69A/S70A/S87A); BCL-2 WT and pCIneo-expressing cells were maintained in selection with 0.4  $\mu$ g/ml G418 (Sigma). For transient silencing of MCL-1 by siRNA, cells were reverse transfected with 10 nM MCL-1 siRNA (no.1: s8583; no.2: s8584; Invitrogen) using Lipofectamine RNAi MAX (Invitrogen) diluted in Optimem medium (Invitrogen) according to the manufacturer's instructions.

**Determination of apoptosis, cell viability and colony formation.** Apoptosis was determined by flow cytometric analysis (FACSCanto II, BD Biosciences, Heidelberg, Germany) of DNA fragmentation of PI-stained nuclei as described previously.<sup>32</sup> The percentage of specific apoptosis was calculated as follows:  $100 \times (\text{experimental apoptosis (\%)} - \text{spontaneous apoptosis (\%)}) /$

$(100 - \text{spontaneous apoptosis (\%)}).$  Spontaneous apoptosis is defined as the amount of DNA fragmentation of untreated cells. Cell viability was assessed by 3-(4,5-dimethylthiazol-2-yl)-2,5-diphenyltetrazolium bromide (MTT) assay according to the manufacturer's instructions (Roche Diagnostics, Mannheim, Germany). For colony assay, cells were treated for 24 (SH-EP) or 36 h (LAN5) before cells were trypsinized, seeded as single cells (200 cells/well) in six-well plates and cultured for additional 14 days before staining with 0.75% crystal violet, 50% ethanol, 0.25% NaCl and 1.57% formaldehyde. The number of colonies was counted under the microscope.

**Western blotting analysis.** Western blotting analysis was performed as described previously<sup>32</sup> using the following antibodies: rabbit anti-caspase-3, rabbit anti-caspase-9 (Cell Signaling, Beverly, MA, USA), rabbit anti-PLK1 (Santa Cruz Biotechnology, Santa Cruz, CA, USA); mouse anti-p21, mouse anti-BCL-2 (BD Biosciences, Franklin Lakes, NJ, USA); mouse anti-murine BCL-2 (Invitrogen); rabbit anti-pH3 (Millipore, Darmstadt, Germany); rabbit anti-MCL-1 (Enzo Life Science, Lörrach, Germany). Mouse anti- $\beta$ -actin (Sigma) and mouse anti-GAPDH (HyTest, Turku, Finland) were used as loading controls. Goat anti-mouse IgG and goat anti-rabbit IgG conjugated to horseradish peroxidase (Santa Cruz Biotechnology) as secondary antibodies and enhanced chemiluminescence were used for detection (Amersham Bioscience, Freiburg, Germany). Alternatively, infrared dye-labeled secondary antibodies and infrared imaging were used for detection (Odyssey imaging system, LI-COR Bioscience, Bad Homburg, Germany). Representative blots of at least two independent experiments are shown.

**Immunoprecipitation.** Immunoprecipitation of active BAX was performed as previously described.<sup>33</sup> Briefly, cells were lysed in CHAPS buffer (1% CHAPS, 150 mM NaCl, 10 mM HEPES pH 7.4) supplemented with a protease inhibitor tablet (Roche, Grenzach, Germany). In all, 1 mg of protein was incubated with 10  $\mu$ g mouse anti-BAX antibody (BD Biosciences) overnight at 4 °C with 20  $\mu$ l pan-mouse IgG Dynabeads (Invitrogen) and washed with CHAPS buffer. BAX was detected using rabbit anti-BAX antibody (Millipore).

**Cell cycle and polyploidy analysis.** Cells were stained with PI, and cell cycle and polyploidy analysis were performed by FlowJo Software (Tree Star Inc., Ashland, OR, USA) according to the manufacturer's instructions.

**Statistical analysis.** Statistical significance was assessed by Student's *t*-test (two-tailed distribution, two-sample, unequal variance). Interaction between Taxol and Bortezomib was analyzed by the CI method based on that described by Chou<sup>34</sup> using the CalcuSyn software (Biosoft, Cambridge, UK). CI < 0.9 indicates synergism, 0.9–1.1 additivity and > 1.1 antagonism.

## Conflict of Interest

The authors declare no conflict of interest.

**Acknowledgements.** We thank Professor WS May (Gainesville, FL, USA) for providing BCL-2 plasmids, Genentech (South San Francisco, CA, USA) for providing MCL-1 plasmids and C Hugenberger for expert secretarial assistance. This work has been partially supported by grants from the Wilhelm Sander-Stiftung and the Deutsche Kinderkrebsstiftung.

1. Maris JM, Hogarty MD, Bagatell R, Cohn SL. Neuroblastoma. *Lancet* 2007; **369**: 2106–2120.
2. Jordan MA, Wilson L. Microtubules as a target for anticancer drugs. *Nat Rev Cancer* 2004; **4**: 253–265.
3. Vermeulen K, Berneman ZN, Van Bockstaele DR. Cell cycle and apoptosis. *Cell Prolif* 2003; **36**: 165–175.
4. Wertz IE, Kusam S, Lam C, Okamoto T, Sandoval W, Anderson DJ *et al*. Sensitivity to antitubulin chemotherapeutics is regulated by MCL1 and FBW7. *Nature* 2011; **471**: 110–114.
5. Harley ME, Allan LA, Sanderson HS, Clarke PR. Phosphorylation of Mcl-1 by CDK1-cyclin B1 initiates its Cdc20-dependent destruction during mitotic arrest. *EMBO J* 2010; **29**: 2407–2420.
6. Frankland-Searby S, Bhaumik SR. The 26S proteasome complex: an attractive target for cancer therapy. *Biochim Biophys Acta* 2012; **1825**: 64–76.

7. Voorhees PM, Orlowski RZ. The proteasome and proteasome inhibitors in cancer therapy. *Annu Rev Pharmacol Toxicol* 2006; **46**: 189–213.
8. de Wilt LH, Kroon J, Jansen G, de Jong S, Peters GJ, Kruyt FA. Bortezomib and TRAIL: a perfect match for apoptotic elimination of tumour cells? *Crit Rev Oncol Hematol* 2013; **85**: 363–372.
9. Brignole C, Marimpietri D, Pastorino F, Nico B, Di Paolo D, Cioni M *et al*. Effect of bortezomib on human neuroblastoma cell growth, apoptosis, and angiogenesis. *J Natl Cancer Inst* 2006; **98**: 1142–1157.
10. Khan T, Stauffer JK, Williams R, Hixon JA, Salcedo R, Lincoln E *et al*. Proteasome inhibition to maximize the apoptotic potential of cytokine therapy for murine neuroblastoma tumors. *J Immunol* 2006; **176**: 6302–6312.
11. Hamner JB, Dickson PV, Sims TL, Zhou J, Spence Y, Ng CY *et al*. Bortezomib inhibits angiogenesis and reduces tumor burden in a murine model of neuroblastoma. *Surgery* 2007; **142**: 185–191.
12. Combaret V, Boyault S, Iacono I, Brejon S, Rousseau R, Puisieux A. Effect of bortezomib on human neuroblastoma: analysis of molecular mechanisms involved in cytotoxicity. *Mol Cancer* 2008; **7**: 50.
13. Armstrong MB, Schumacher KR, Mody R, Yanik GA, Opari AW Jr, Castle VP. Bortezomib as a therapeutic candidate for neuroblastoma. *J Exp Ther Oncol* 2008; **7**: 135–145.
14. Michaelis M, Fichtner I, Behrens D, Haider W, Rothweiler F, Mack A *et al*. Anti-cancer effects of bortezomib against chemoresistant neuroblastoma cell lines in vitro and in vivo. *Int J Oncol* 2006; **28**: 439–446.
15. Valentiner U, Haane C, Nehmann N, Schumacher U. Effects of bortezomib on human neuroblastoma cells in vitro and in a metastatic xenograft model. *Anticancer Res* 2009; **29**: 1219–1225.
16. Naumann I, Kappler R, von Schweinitz D, Debatin KM, Fulda S. Bortezomib primes neuroblastoma cells for TRAIL-induced apoptosis by linking the death receptor to the mitochondrial pathway. *Clin Cancer Res* 2011; **17**: 3204–3218.
17. Unterkircher T, Cristofanon S, Vellanki SH, Nonnenmacher L, Karpel-Massler G, Wirtz CR *et al*. Bortezomib primes glioblastoma, including glioblastoma stem cells, for TRAIL by increasing tBid stability and mitochondrial apoptosis. *Clin Cancer Res* 2011; **17**: 4019–4030.
18. Tamura D, Arai T, Tanaka K, Kaneda H, Matsumoto K, Kudo K *et al*. Bortezomib potentially inhibits cellular growth of vascular endothelial cells through suppression of G2/M transition. *Cancer Sci* 2010; **101**: 1403–1408.
19. Strebhardt K. Multifaceted polo-like kinases: drug targets and antitargets for cancer therapy. *Nat Rev Drug Discov* 2010; **9**: 643–660.
20. Hans F, Dimitrov S. Histone H3 phosphorylation and cell division. *Oncogene* 2001; **20**: 3021–3027.
21. Janssen A, Medema RH. Mitosis as an anti-cancer target. *Oncogene* 2011; **30**: 2799–2809.
22. Lu Z, Hunter T. Ubiquitylation and proteasomal degradation of the p21(Cip1), p27(Kip1) and p57(Kip2) CDK inhibitors. *Cell Cycle* 2010; **9**: 2342–2352.
23. Deng X, Gao F, Flagg T, May WS Jr. Mono- and multisite phosphorylation enhances Bcl2's antiapoptotic function and inhibition of cell cycle entry functions. *Proc Natl Acad Sci USA* 2004; **101**: 153–158.
24. Willmott S, Wagner SD. Post-transcriptional and post-translational regulation of Bcl2. *Biochem Soc Trans* 2010; **38**: 1571–1575.
25. Deng X, Gao F, May WS Jr. Bcl2 retards G1/S cell cycle transition by regulating intracellular ROS. *Blood* 2003; **102**: 3179–3185.
26. Mazel S, Burtrum D, Petrie HT. Regulation of cell division cycle progression by bcl-2 expression: a potential mechanism for inhibition of programmed cell death. *J Exp Med* 1996; **183**: 2219–2226.
27. Vega MI, Martinez-Paniagua M, Jazirehi AR, Huerta-Yepez S, Umezawa K, Martinez-Maza O *et al*. The NF-kappaB inhibitors (bortezomib and DHMEQ) sensitise rituximab-resistant AIDS-B-non-Hodgkin lymphoma to apoptosis by various chemotherapeutic drugs. *Leuk Lymphoma* 2008; **49**: 1982–1994.
28. Dong QG, Sclabas GM, Fujioka S, Schmidt C, Peng B, Wu T *et al*. The function of multiple I-kappaB: NF-kappaB complexes in the resistance of cancer cells to Taxol-induced apoptosis. *Oncogene* 2002; **21**: 6510–6519.
29. Bruning A, Burger P, Vogel M, Rahmeh M, Friese K, Lenhard M *et al*. Bortezomib treatment of ovarian cancer cells mediates endoplasmic reticulum stress, cell cycle arrest, and apoptosis. *Invest New Drugs* 2009; **27**: 543–551.
30. Fanucchi MP, Fossella FV, Belt R, Natale R, Fidiis P, Carbone DP *et al*. Randomized phase II study of bortezomib alone and bortezomib in combination with docetaxel in previously treated advanced non-small-cell lung cancer. *J Clin Oncol* 2006; **24**: 5025–5033.
31. Loeder S, Fakler M, Schoeneberger H, Cristofanon S, Leibacher J, Vanlangenakker N *et al*. RIP1 is required for IAP inhibitor-mediated sensitization of childhood acute leukemia cells to chemotherapy-induced apoptosis. *Leukemia* 2012; **26**: 1020–1029.
32. Fulda S, Sieverts H, Friesen C, Herr I, Debatin KM. The CD95 (APO-1/Fas) system mediates drug-induced apoptosis in neuroblastoma cells. *Cancer Res* 1997; **57**: 3823–3829.
33. Hacker S, Dittrich A, Mohr A, Schweitzer T, Rutkowski S, Krauss J *et al*. Histone deacetylase inhibitors cooperate with IFN-gamma to restore caspase-8 expression and overcome TRAIL resistance in cancers with silencing of caspase-8. *Oncogene* 2009; **28**: 3097–3110.
34. Chou TC. The median-effect principle and the combination index for quantitation of synergism and antagonism. In: Chou TC (ed). *Synergism and Antagonism in Chemotherapy*. Academic Press: San Diego, CA, USA, 1991. pp 61–102.



**Cell Death and Disease** is an open-access journal published by Nature Publishing Group. This work is licensed under a Creative Commons Attribution-NonCommercial-NoDerivs 3.0 Unported License. To view a copy of this license, visit <http://creativecommons.org/licenses/by-nc-nd/3.0/>

Supplementary Information accompanies this paper on Cell Death and Disease website (<http://www.nature.com/cddis>)